Academic Journal of Science and Technology
ISSN: 2771-3032 | Vol. 3, No. 2, 2022

Study on the Cone Angle of Sliding Sleeve Ball Seat in Open Hole Staged Ball Throwing Fracturing

Ruolan Li[1], Dongsheng He[2] and Lang Xiong[2]

[1]School of Chengdu, Southwest Petroleum University, Sichuan 610000, China
[2]Company of Karamay, PetroChina Western Drilling Downhole Operation Company, Xinjiang 834000, China

Abstract: In the ball type fracturing sliding sleeve, the contact surface between the ball socket and the fracturing ball is the most vulnerable part to failure. Once the contact surface fails, the sealing of the fracturing sliding sleeve will fail, the fracturing fluid will leak, and finally the fracturing will fail. The contact condition between the ball socket and the fracturing ball is mainly determined by the cone angle of the ball socket. In order to improve the contact condition between the ball socket and the fracturing ball as much as possible, and extend the service life of the sliding sleeve, based on fluid erosion and finite element structural analysis, this paper has carried out the analysis of the cone angle of the fracturing sliding sleeve. Firstly, the erosion of the ball seat is analyzed, and the erosion rate of the ball seat under different cone angles is obtained. The conclusion is that the erosion rate of the ball seat is proportional to the cone angle of the ball seat. Combined with the working conditions of the ball socket fracturing, the finite element analysis of the ball socket structure is carried out, and the stress conditions of different cone angles are compared. Finally, combined with the erosion rule and force analysis of the ball socket, the optimal cone angle of the ball socket is 20 °. When the cone angle of the ball socket is 20 °, the force of the ball socket meets the strength requirements of the ball socket, and can obtain a higher service life.

Keywords: Fracturing sliding sleeve, Ball seat cone angle, Erosion rate, Stress, Contact stress.

1. Introduction

With the deepening and development of oil and gas exploration and development process, low permeability, shale, tight and other difficult to exploit oil and gas resources account for an increasing proportion in exploration and development. Low permeability oilfields are widely distributed in China, especially in Sichuan and Chongqing areas. Shale gas productivity is low due to its large rock density, small porosity, low permeability and complex geological conditions [1-4]. At present, the main method to exploit shale gas is multi-stage fracturing technology for horizontal wells. Due to the long wellbore of horizontal wells, casing deformation is very easy to occur during multi-stage fracturing. In addition, hydraulic fracturing technology has great limitations when facing wells with complex structures and complex formations [5-9]

In recent years, the open hole staged fracturing technology for horizontal wells is a new technology to exploit unconventional oil and gas fields, which has broad application prospects and economic benefits. It is mainly composed of multiple groups of open hole packers and multi-stage fracturing sliding sleeves, which conduct staged fracturing for low permeability long horizontal sections [10-16]. In the open hole staged fracturing process, the sealing performance of the fracturing sliding sleeve directly determines the success or failure of the fracturing, and the ball seat is the key component directly involved in the fracturing sealing. The failure of the ball seat seal may lead to the failure of the entire multi-stage fracturing. There are two main reasons for the seal failure of the ball seat: one is the plastic deformation of the ball seat caused by excessive stress, which leads to the seal failure; Second, the fracturing fluid containing proppant continuously impacted the conical surface of the ball socket, causing erosion wear of the conical surface of the ball socket [17]. Among them, the erosion of fracturing fluid on the cone surface of the ball seat is the main reason for the failure of the ball seat [18]. From these two aspects, this paper uses Ansys finite element simulation and Fluent erosion analysis to simulate the working conditions under different ball seat cone angles. Based on the structural data of the sliding sleeve structure in the subject, in this design, the diameter of the fracturing ball D=84.5mm, the design inner diameter of the ball seat after shrinkage is d=76.5mm, and its diameter difference Δ=D-d=8mm. With this parameter, the optimal fracturing ball seat cone angle is studied.

2. Pressure Bearing Analysis of Ball Seat Structure

During the whole fracturing process of fracturing sliding sleeve, the most severe working condition is that the fracturing ball is set on the ball seat and the fracturing fluid is used to fracturing the formation. At this time, the differential pressure between the upper and lower parts of the ball socket reaches the maximum value. To ensure that the fracturing sliding sleeve can complete the sealing work, it is necessary to make a specific analysis of the working conditions of the ball socket. The correct setting of fracturing ball must meet the following three requirements:

The fracturing ball must be seated on the conical surface of the ball seat;

The ball seat shall meet the structural strength requirements;

The fracturing ball shall not be self-locking with the ball socket.

2.1. Ensure that the fracturing ball is seated on the conical surface of the ball seat

According to the operation of the ball socket during fracturing, the contact relationship between the fracturing ball and the ball socket is shown in Figure 1:

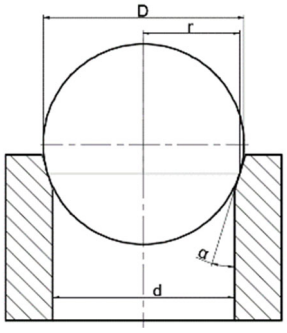

Figure 1. Fracturing Ball Set on Ball Seat

To seat the fracturing ball on the conical surface of the ball seat:

$$2r = D\cos\alpha > d \tag{1}$$

Where, D is the diameter of sealing ball, 84.5mm; D is the shrinkage diameter of the ball seat, taking 76.5mm; R is the radius of the fracturing ball section on the setting section.

The taper angle of the ball seat can be calculated according to the above formula α< arccos d/D=25.13°.

2.2. Ensure that the fracturing ball does not lock with the ball socket

After fracturing, the fracturing ball needs to disengage from the ball seat and automatically discharge the sliding sleeve under the action of formation pressure P. The fracturing ball backflow is divided into two stages. First, after the fracturing fluid pressure is removed, the fracturing ball automatically disengages from the ball socket; Then the fracturing ball reversely discharges the sliding sleeve under the formation pressure. In the first stage, the upper pressure of the fracturing ball disappears, the fracturing ball breaks away from the socket by elastic deformation, and the fracturing ball keeps balance under the action of positive pressure and friction [19]. The relationship between the two forces is: N= μ · f, assuming that the fracturing ball is an elastomer, there are:

$$N = \mu \backslash f \qquad N' = N \tag{2}$$

Where, N is the reaction force of the ball seat to the fracturing ball after fracturing; N ^ 'is the reaction force between the ball seat and the fracturing ball during fracturing; μ Is the friction coefficient between the ball seat and fracturing; F is the friction between the ball seat and the fracturing ball.

According to the above formula, it can be deduced that the half cone angle of the fracturing ball that can automatically separate from the ball socket when the fracturing fluid pressure is removed is

$$\alpha = \arctan\mu \tag{3}$$

Where, α Is the cone angle of the ball seat.

The fracturing ball used in this design is a low-density composite ball, and the friction coefficient should be 0.3. Therefore, in order to prevent the fracturing ball from self-locking with the ball seat after the fracturing fluid pressure is removed, the half cone angle of the ball seat α> arctan(0.3)=16.69°.

In conclusion, to meet the requirements, the cone angle of the ball seat should be selected between 16.69 ° and 25 °

3. Ball Seat Erosion Analysis

The fracturing fluid contains a large number of solid particles. Under the continuous impact of the fracturing fluid, the ball seat will appear pitting, pitting and other phenomena, which may eventually lead to the seal failure of the ball seat [20]. In order to reduce the erosion of the ball seat as much as possible and optimize the cone angle of the ball seat, this paper calculates the erosion wear of the ball seat with different cone angles based on hydrodynamics and cutting deformation theory.

The sand carrying fracturing fluid is a solid-liquid two-phase flow. Assuming that the fluid is incompressible, DMP discrete phase model is used to simulate the flow field movement inside the sliding sleeve.

3.1. Establishment of Ball Seat Erosion Wear Equation

When the discrete phase model is used, the wall wear rate R must be set_ Erosion [21], which is defined as:

$$R_{\text{erosion}} = \sum_{p=1}^{N} \frac{m_p C\left(d_p\right) f\left(\alpha\right) V_p^{\,b(v_p)}}{A_{face}} \tag{4}$$

Where, m_p is the mass flow of proppant; C is the function of proppant particle diameter, taken as 1.9×10^{-9}; $V_p^{\,b(V_P)}$ Is the impact velocity function, taken as 2.3; A_{face} is the erosion area; $f(\alpha)$ Is a function of impact angle.

According to Finnie's classical cutting theory of plastic materials [22], a theoretical model of erosion wear of ball seats is established. The impact angle function of ball seats is:

$$f\left(\alpha\right) = \sin\left(2\alpha\right) - 3\sin^2\alpha \qquad (\alpha \le 18.43°) \tag{5}$$

$$f\left(\alpha\right) = \cos^2\alpha / 3 \qquad (\alpha \ge 18.43°) \tag{6}$$

According to the calculation formula of impact angle function, the impact angle function of each cone angle spherical seat wall is shown in Table 1:

Table 1 Impact Angle of Ball Seat Wall

3.2. Calculation of ball socket erosion of ball throwing sliding sleeve

Assume that the density of fracturing fluid is 1400 kg/m3, the proppant density is 1800 kg/m3, the proppant volume fraction is 10%, the particle size is 0.6mm, the fracturing fluid flow is Q=5m ^ 3/min, the formation pressure is 60MPa, and the fracturing fluid viscosity is μ Take 0.1, the diameter of the front end of the model is the inner diameter of the fracturing sliding sleeve, take 116mm, the lower end of the model is the shrinkage diameter of the ball seat, take 76.5mm, then the inlet flow rate is: v=Q／A=7.89m/s, and the mass flow rate of the proppant is: m=0.1 (Q ／ 60) ρ= 15kg/s, Reynolds

coefficient of fracturing fluid: Re= ρ vd/μ= （1400 × seven point eight nine × 0.116)/(0.1=12813>10000), the fluid is in a completely turbulent state [23], so the turbulence model is adopted. The turbulence boundary conditions are turbulence intensity and hydraulic diameter, and the turbulence intensity is I=0.16 [Re] ^ (- 1/8)=4.91%.

In order to make the fracturing fluid reach a stable state when reaching the ball socket, the ball socket model extends forward and backward for 200mm respectively. The ball socket model is divided into grids by hexahedral elements, and the boundary layer grid is divided on the wall. The model and grid are shown in Figure 2.

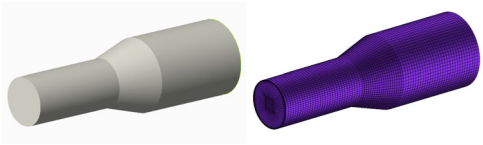

Figure 2. Ball seat erosion model and grid division

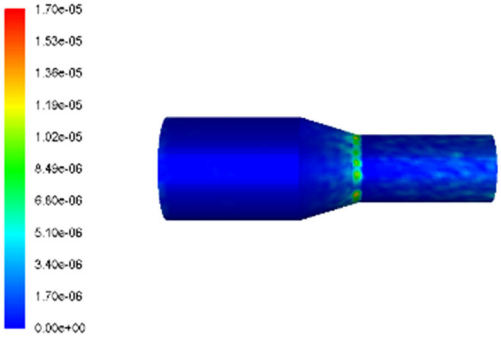

Figure 3. Erosion rate diagram at 17 ° cone angle

Firstly, the erosion analysis is carried out for the ball seat model with a cone angle of 17 °. The erosion wear results of the ball seat are shown in Figure 3.

It can be seen from the erosion rate diagram that the erosion phenomenon is mainly distributed at the conical surface of the ball seat and the rear runner of the ball seat. The erosion wear in the lower area of the conical surface of the ball seat is the most serious, with the maximum erosion wear rate of 1.70 × 10-5kg/(m2 · s), the erosion of the ball seat with the remaining cone angle of 18 ° to 25 ° is shown in Figure 4:

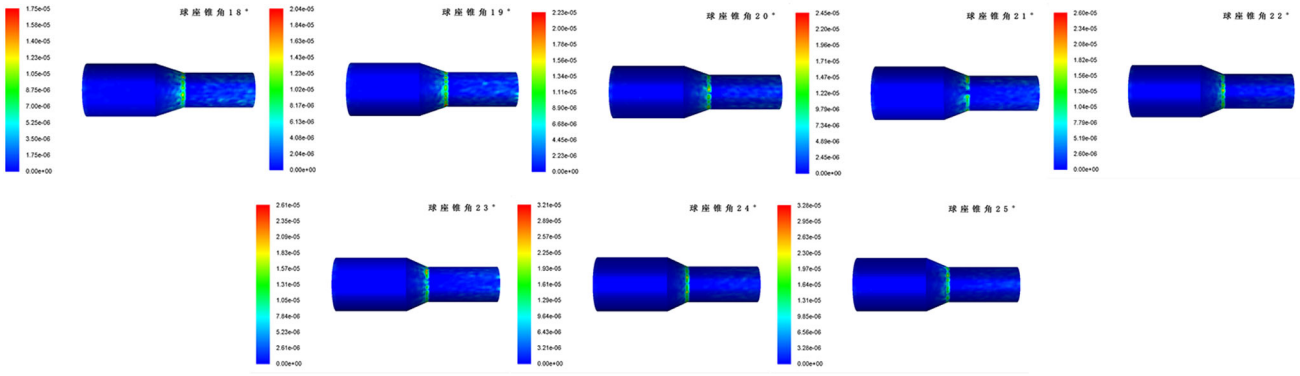

Figure 4. Erosion Rate Diagram of Cone Angle 18 °~25 °

The erosion rate results of each cone angle of the ball seat can be obtained through the erosion wear analysis of the ball seats with different cone angles, as shown in Table 2:

Table 2. Erosion Rate of Each Cone Angle

Ball seat cone angle / °	17	18	19	20	21	22	23	24	25
erosion rate /×10^{-5}kg/(m^2·s)	1.70	1.75	2.04	2.23	2.45	2.60	2.61	3.21	3.28

It can be seen from the ball seat erosion rate diagram that the places where the ball seat is most seriously eroded are basically the same, and the erosion rate increases with the increase of the cone angle of the ball seat. Therefore, from the aspect of socket erosion, the cone angle of the socket should be as small as possible to reduce socket erosion and extend the service life of the socket.

4. Stress Analysis of Ball Socket Structure

4.1. Finite element model and grid division of ball socket structure

According to the specific working conditions during fracturing, the fracturing sliding sleeve is simplified. The design adopts a petal type ball seat structure, which is composed of six lobes when the ball seat is opened. Therefore, the model uses a 1/6 calculation model to grid the model. In order to obtain a higher quality grid, this paper uses Hypermesh as the preprocessor, and then uses the Ansys solver for calculation and analysis. The ball seat structure model and grid are shown in Figure 5.

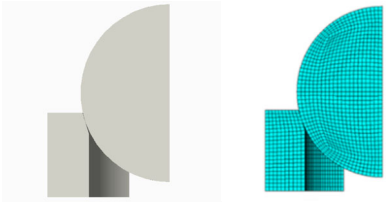

Figure 5. Ball socket model and grid division

4.2. Model materials and boundary conditions

The fracturing sliding sleeve is made of 42CrMo, and the fracturing ball is made of low-density composite materials. The material performance parameters are shown in Table 3:

Table 3. Material Parameters of Slip Sleeve and Fracturing Ball

Material Science	Elastic modulus /GPa	Poisson's ratio	Yield strength /MPa	Tangent modulus /GPa	Density /kg.m-3
Ball socket	212	0.28	930	6.1	7830
Fracturing ball	90	0.33	355	1.9	1400

The boundary conditions are set as follows:

(1) The lower end of the model is completely fixed;

(2) The contact surface between the fracturing ball and the ball seat is set up to contact;

(3) Apply 50MPa pressure on the upper surface of the fracturing ball and the upper surface of the ball socket at the same time; A pressure difference of 50MPa is formed between the upper and lower parts of the ball seat.

4.3. Finite element analysis results of ball socket structure

The Von Mises stress of the ball socket and the contact stress of the contact surface under different cone angles are analyzed respectively. The stress nephogram is shown in the following figure:

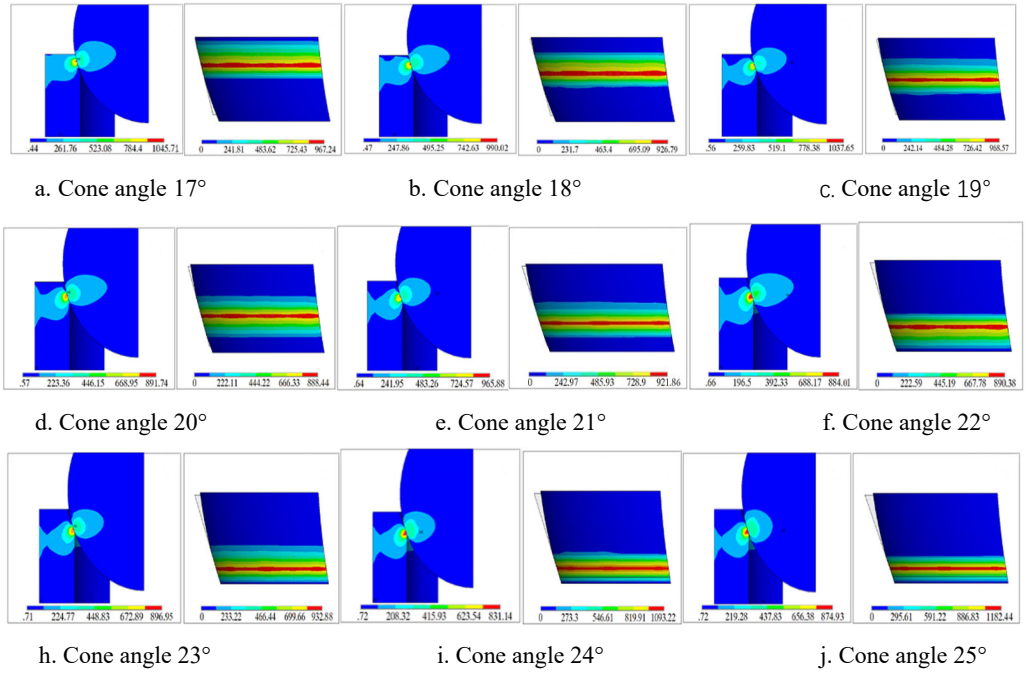

a. Cone angle 17° b. Cone angle 18° c. Cone angle 19°

d. Cone angle 20° e. Cone angle 21° f. Cone angle 22°

h. Cone angle 23° i. Cone angle 24° j. Cone angle 25°

Figure 6. Stress nephogram of ball socket with cone angle of 17 °~25 °

According to the finite element analysis of the ball socket structure with cone angles from 17 ° to 25 °, as shown in Figure 6, as the cone angle of the ball socket increases, the contact position between the fracturing ball and the ball socket also moves downward. The maximum Von Mises stress and contact surface contact stress of the ball socket structure under each cone angle are shown in Table 4:

Table 4. Von Mises Stress and Contact Stress of Ball Seat Structure with Cone Angle of 17 °~25 °

Cone Angle/ °	17	18	19	20	21	22	23	24	25
Von-mises Stress/MPa	1045.71	990.02	1037.65	891.74	965.88	884.01	896.95	831.14	874.93
Contact Stress/MPa	967.24	926.79	968.57	888.44	921.86	890.38	932.88	1093.22	1182.44

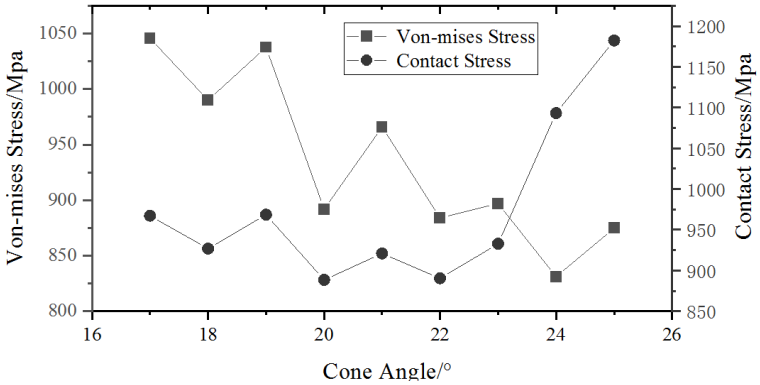

Figure 7. Von Mises Stress and Contact Stress Diagram of Ball Seat Structure with Cone Angle of 17 °~25 °

It can be seen from the finite element analysis results of the ball seat structure shown in Figure 7 that in the Von Mises stress analysis of the ball seat, the Mises stress generally decreases with the increase of the cone angle, and there are five cases where the stress does not exceed the yield strength of the ball seat 930MPa, namely, the cone angle of the ball seat is 20 °, 22 °, 23 °, 24 ° and 25 °. With the increase of cone angle, the contact stress decreases first and then increases. There are four cases that do not exceed the yield strength of the socket, namely, the cone angle of the socket is 18 °, 20 °, 21 ° and 22 °. To sum up, there are two cases where the cone angle of the ball seat meets the structural strength requirements of the ball seat, namely, the cone angle is 20 ° and the cone angle is 22 °.

5. Summary

According to the stress analysis of the ball socket structures with different cone angles, the cone angles of the full ball socket structure strength are 20 ° and 22 °. However, combined with the erosion analysis of the ball socket, the erosion strength of the ball socket with a cone angle of 20 ° is less than that of the ball socket with a cone angle of 22 °. Therefore, the ball socket structure with a cone angle of 20 ° has a higher erosion life than that of the ball socket structure with a cone angle of 22 °. Therefore, under the condition that the cone angles of the two types of sockets meet the structural strength, 20 ° with lower erosion strength is selected as the selection standard of the cone angle of the socket.

Acknowledgment

Supported by the "13th Five Year Plan" National Science and Technology Major Special Project "Risk Assessment of Deepwater Testing and Research on Well Completion and Wellbore Integrity" (2016ZX05028001-006) and "Development of Non differential Ball Slippers" of Western Drilling

References

[1] Jiang Y X. Fracturing Technology and Case Analysis of Complex and Difficult to Produce Oil and Gas Reservoirs[M]. Beijing:Sinopec Press.

[2] Hao S Y, Zhang L. Development Technology and Management of Low Permeability Oilfield[M]. Beijing: Petroleum Industry Press, 2012.

[3] Yan C Z. Papers on Low Permeability Oilfield Development[M]. Beijing: Petroleum Industry Press, 2008.

[4] Li C Q. Application of staged fracturing in horizontal wells in the development of ultra-low permeability reservoirs[J]. Journal of Southwest Petroleum University (Natural Science Edition), 2001,33 (6): 85-88.

[5] Wang R. Analysis of factors influencing volume fracturing effect of horizontal wells in tight reservoirs[J]. Special Oil and Gas Reservoirs, 2015, 22 (2): 126-128.

[6] Wang H, Liao X W, Zhao X L, et al. Research progress of reservoir volume reconstruction simulation technology for unconventional oil and gas reservoirs[J]. Special Oil and Gas Reservoirs, 2014, 21 (2): 8-15.

[7] Pu J W, Luo M L, Wen Q Z, et al. Finite Discrete Element Analysis on Fracturing of Tight Sandstone Reservoir[J]. Special oil and gas reservoirs, 2018.

[8] Xi Y, Li J, Liu G H, et al. Overview of Casing Deformation in Multistage Fracturing of Shale Gas Horizontal Wells[J]. Special oil and gas reservoirs, 2018.

[9] Tong S K,Gao D L. Basic research progress and development suggestions on hydraulic fracturing[J]. Petroleum drilling and production process, 2018.

[10] Bi M, Hu Y M, Zhu L A, et al. Research and application of geological model of staged fracturing for horizontal wells in tight gas reservoirs and optimization of cost reduction and benefit increase[J]. Drilling and production process, 2018,41 (5): 59-62.

[11] Ling Y, Li X W. New progress in fracturing technologies for tight sandstone gas reservoirs in the Sulige Gas Field,Ordos Basin[J]. Natural gas industry, 2014, 34 (11): 66-72.

[12] Li X W, Ling Y, Ma X, et al. New Development of Fracturing Technology for Low Permeability Sandstone Gas Reservoirs in Changqing Gas Area -- Taking Sulige Gas Field as an Example[J]. Natural gas industry, 2011, 31 (2): 20-24.

[13] Cheng P.Drilling and Completion Engineering[D]. Beijing: Petroleum Industry Press, 2005.

[14] Mu L J，Ma X，Zhang Y M，et al. Evaluation of multistage fracturing by hydrajet，swellable packer，and compressive packer techniques in horizontal openhole wells[R]. SPE 153328，2012.

[15] Li B, Zheng X, Zhang Z P, et al. Study on sealing of ball sliding sleeve in open hole staged fracturing[J]. Journal of Applied Mechanics, 2017,34 (6): 1134-1139.

[16] Xun H X, Shi X, Ji M S. Effect of Packers on the Initiation Pressure of Open Hole Staged Fracturing in Shale Gas Horizontal Wells. Proceedings of 2017 National Natural Gas Academic Annual Conference[C]. 2017.

[17] Liu F C.Design method of horizontal well fracturing[D]. Xian: Xian University of Petroleum, 2011.

[18] Qin J L, Wu J H, Cui X J, et al. Key Technology on Ball-Activated Sleeve for Open Hole Staged Fracturing[J]. Petroleum Drilling Technology, 2014, 42 (5): 52-56.

[19] Feng C Q, Zhang H G, Zhao F X, et al. Force Analysis of Layered Fracture Sliding Sleeve and Seal Ball[J]. Petroleum Machinery, 2013, 41 (2): 75-78.

[20] Li Q, Dong S X, Lu Z X, et al. Research on Erosion Wear ang Evaluation Methods of Sliding Sleeve Tee[J]. Lubrication and sealing, 2016,41 (7): 116-119.

[21] Fluent I. Fluent user's guide[M].Fluent Inc,2006.

[22] Forder A, Thew M, Harrison D. A numerical investigation of solid particle erosion experienced within oilfield control valves[J]. Wear,1998,216(2):184-193.

[23] Wang L, Cheng G Z. Engineering Fluid Mechanics[M]. Beijing: Petroleum Industry Press, 2007.